Lab on a Chip

Cite this: *Lab Chip*, 2012, **12**, 1594

www.rsc.org/loc

COMMUNICATION

Mesh-integrated microdroplet array for simultaneous merging and storage of single-cell droplets†

Eujin Um,[a] Eugene Rha,[b] Su-Lim Choi,[b] Seung-Goo Lee*[b] and Je-Kyun Park*[a]

Received 19th December 2011, Accepted 23rd February 2012
DOI: 10.1039/c2lc21266h

We constructed a mesh-grid integrated microwell array which enables easy trapping and consistent addition of droplets. The grid acts as a microchannel structure to guide droplets into the microwells underneath, and also provides open access for additional manipulation in a high-throughput manner. Each droplet in the array forms a stable environment of pico-litre volume to implement a single-cell-based assay.

To study genuine responses or secretions from single cells or cell-to-cell communications while excluding the effects of neighboring cells, each cell has to be isolated in a small volume. Conventional tools such as microplates usually handle a minimum volume of ~10 μL which is still large compared with a single-cell volume of ~1 pL; thus repetitive and inefficient dilution processes in multiple wells are required. To induce proper cell behaviors with low cell numbers, controlling the number of cells per unit confinement is important, and microfabrication and microfluidic tools can help control spatial proximity of cells and the isolation process.[1–3] Microfabricated well arrays allow for a large number of wells per unit area and confinement of single cell compatible sizes.[4–6] There are still challenges in the controlled isolation of microbes such as *Escherichia coli* (*E. coli*) into single-cell units due to their small sizes and irregular shapes. There are also difficulties in accessing individual wells for different treatments and recovery of cells.

An alternative method to create cell microconfinements is the formation of microdroplets from two-phase fluids. Microdroplets of pico- to nanolitre volumes are capable of enclosing various biological matter.[7,8] Unlike solid wells, they are a more active system, and can move or stop, split or merge with others, and select different paths for sorting at timed intervals.[9–11] As illustrated in Fig. 1, to conduct a biological assay, multiple droplet manipulation steps are required, including droplet generation with single cells, stable storage, and merging with additional droplets to activate the reaction or supplement medium. It is also desirable to be able to perform further processes such as changing the continuous oil phase of different constituents or recovery of droplets to recollect the selected cells for further analysis. Although each method of droplet manipulation has been successfully demonstrated, difficulty in integrating these steps into a whole system has limited the applicability of droplet technology for complete biological assays.

The integration of an array structure in a closed microchannel in order to stably store droplets has been accomplished,[12–15] but a technique for the repetitive addition of droplets or the selection of specific droplets in a closed channel by inspection has not yet been developed. There is a method for transferring droplets to and from each functional module with the help of a surfactant;[16] however, without physical boundaries for trapping droplets, it is difficult to keep them in fixed positions during an extended time for tracking and inspection. To apply physical boundaries, a sophisticated design is

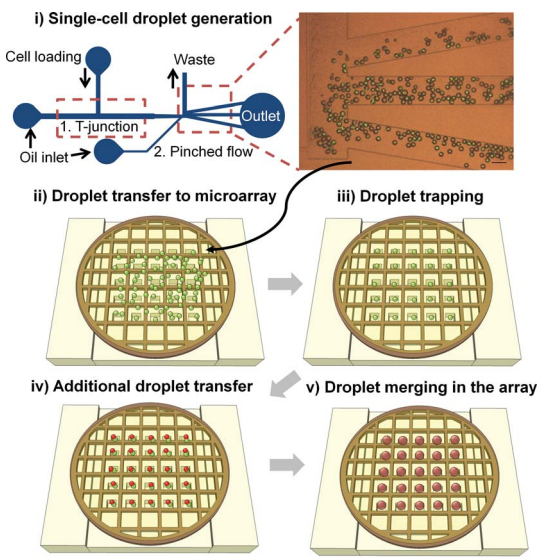

Fig. 1 Schematic representation of the manipulation of microdroplets in the microarray. The process includes: (i) droplet generation from an independent microchannel for single-cell encapsulation. The scale bar in the microscopic image is 50 μm; (ii) transfer of droplets onto the mesh-integrated microwell array; (iii) migration of droplets into the wells and removal of untrapped droplets with oil flow; (iv) trapping of the second droplets; (v) oil change to induce droplet merging.

[a]*Department of Bio and Brain Engineering, Korea Advanced Institute of Science and Technology (KAIST), 291 Daehak-ro, Yuseong-gu, Daejeon, 305-701, Republic of Korea. E-mail: jekyun@kaist.ac.kr; Fax: +82-42-350-4310; Tel: +82-42-350-4315*

[b]*Systems and Synthetic Biology Research Center, Korea Research Institute of Bioscience and Biotechnology (KRIBB), 125 Gwahak-ro, Yuseong-gu, Daejeon, 305-806, Republic of Korea. E-mail: sglee@kribb.re.kr; Fax: +82-42-860-4489; Tel: +82-42-860-4373*

† Electronic supplementary information (ESI) available. See DOI: 10.1039/c2lc21266h

necessary to account for the behavior of droplets, which are highly sensitive to small perturbations such as pressure, flow rate, and the number of droplets. This hinders combinations of functioning modules and droplet manipulation. Practically, capturing droplets at sizes of tens of micrometres for containing single cells is especially difficult, because it requires more energy to deform and trap small droplets. The removal of unwanted droplets trapped in the array is also problematic.

Our research focuses on the development of a microstructure for stably inserting droplets into microwells with high efficiency that still provides an open system allowing easy access to the contents and integration with other microfluidic modules. A microwell array system should be applicable for screening microbial cells by incubation and inspection for several hours. After single-cell droplets of 10–15 pL volume (~30 μm in diameter) are generated, they could be transferred to fixed positions for merging with additional droplets and for inspection (Fig. 1).

Prior to creating a droplet array, single-cell droplets are generated from an independent device. With a conventional droplet-generating method, the proportion of single-cell containing droplets is usually less than 30%.[7,16–18] The chance of two different cells co-localizing in one droplet for reaction by droplet-merging is even lower. To enhance the single-cell encapsulation efficiency, we used a pinched-flow channel for the secondary breakup of droplets (Fig. 1 and see ESI, Fig. S1†), thereby reducing stochastic loading of the cells.[19] The large droplets first generated from the T-channel are compactly loaded with a high concentration of cells; these droplets then break for a second time at the pinched-flow channel, creating smaller droplets 30 μm in diameter, which is compatible to containing one microbial cell (initially in a medium with 1×10^8 to 2×10^8 cells per mL). By initially loading a high concentration of cells into large droplets, the problems of uneven distribution of cells in a microchannel and cell adhesion to the wall are greatly reduced. With this design, approximately 50% of droplets collected at the outlet would be expected to contain a single *E. coli* cell.

Structurally, the array consists of a flat metal grid aligned above the poly(dimethylsiloxane) (PDMS) microwells separated by spacers (see ESI, Fig. S2† and Fig. 2a). The grid structure allows the free flow of oil to pass through, as it draws and guides droplets into the wells aligned beneath (Fig. 2b). Without the grid, droplets in the oil would follow the bulk flow outside of the microwells and would not enter the narrow wells. The vertical velocity (see w in Fig. 2b) toward the wells is almost zero near the surface opening of the wells, and air will start to fill the wells as the oil permeates into PDMS or evaporates. However, the mesh-grid above the microwells acts as a microchannel structure to hold a thin film of oil, instead of bulk flow, in the space (see s in Fig. 2b) between the grid and the PDMS array. When droplets fall through the grid following the oil stream, they will move directly into the wells because the space between the grid and the PDMS array is set to be smaller than the droplets. They tend to stay in the wells, where their shape deformation can be minimized, thus reducing the surface energy. After droplets are settled in the wells, residual droplets can be flushed out with additional oil flow. The oil phase used throughout the whole process is mineral oil, with a density of 0.84 g mL^{-1} (Sigma-Aldrich, St. Louis, MO, USA).

As droplets for single-cell encapsulation are 30 μm in diameter, a mesh grid (Electron Microscopy Science, PA, USA) with a hole width of 43 μm and a wire dimension of 20 μm was chosen to allow free passage of the droplets and oil. Each microwell in the array was designed to have a width and depth of 40 μm each, and wells were spaced 23 μm apart. The number of well arrays is limited only by the size of the microgrid. Here, we used 900 wells on a 2 mm × 2 mm microgrid. The height of the spacers, s, between the grid and the array was 25 μm. Droplets of 40 μm diameter filled approximately 95% of the microwell array, and droplets of 30 μm diameter resulted in approximately 80% single-droplet occupancy (Fig. 2c and d).

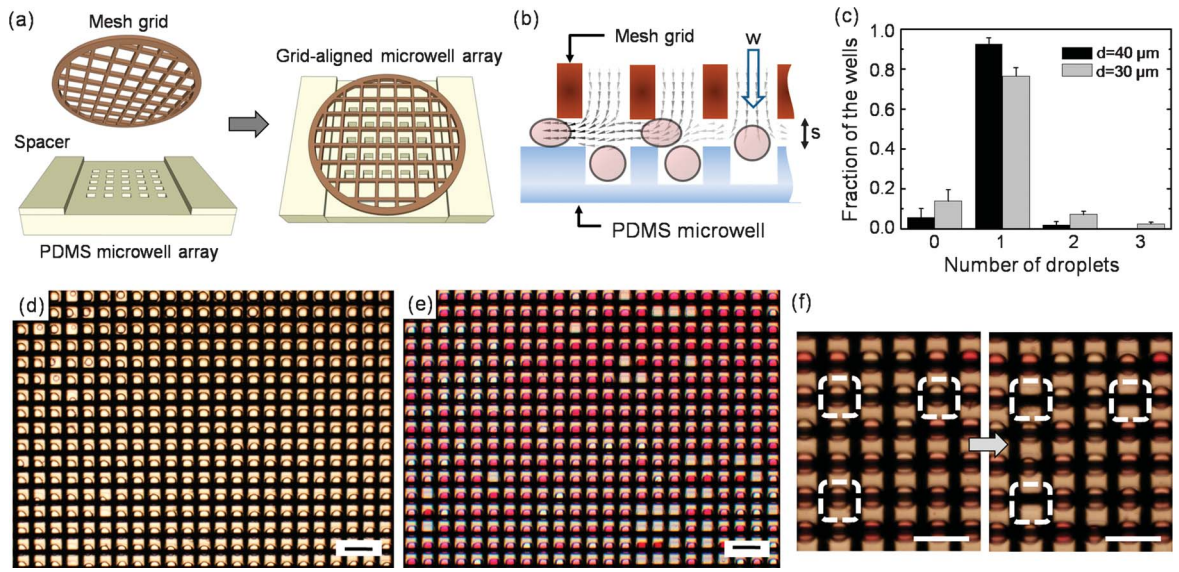

Fig. 2 Operation of the mesh-integrated microwell array. (a) The mesh structure is aligned over the microwell array and separated by spacers. (b) Side view of the mesh-integrated microwell array, which guides the droplet path and allows easy oil change and removal of untrapped droplets. (c) Graph showing the fraction of wells according to the number of occupying droplets. More than 98% of the wells trapped one droplet when the well size was comparable to the droplet diameter. (d–f) Microscopic images of the mesh-integrated microwell showing (d) trapping of single droplets, (e) addition of the second droplets (colored with red dye) (see ESI, Video S1†), and (f) selective removal of three droplets using a glass capillary tube (see ESI, Video S2†). All scale bars are 100 μm.

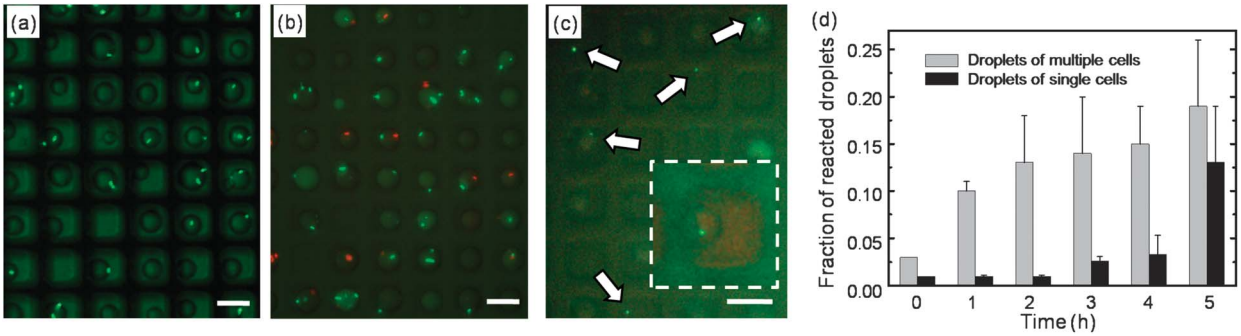

Fig. 3 Mesh-integrated array with cell-containing droplets. (a) First, trapping of droplets with green fluorescent cells. (b) Second, addition of droplets with red fluorescent cells to demonstrate co-existence of different cells from separate droplets. (c) Application of droplets for single-cell-based assays by encapsulating enzyme-producing cells and the reporter cells. White arrows indicate green fluorescence appearing from the reporter cells in the presence of the enzyme activity, with the white dashed line showing the enlarged image of the reacted droplet. (d) Fraction of reacted droplets in the array when the numbers of both enzyme-producing cells and the reporter cells per droplet were controlled to be multiple (5–10 cells) or single. All scale bars are 50 μm. The mesh grid was removed in (b) and (c) for better inspection of cells.

In most applications, droplets are stabilized by a high percentage of surfactant, which hinders droplet-merging; coincidence of the time and location of droplets alone is not sufficient.[11] Because the mesh grid provides an open structure to the microwells, merging events of additional droplets could easily be performed using the chemical demulsification method, instead of integrating complex hydrodynamic merging channels or active components such as electrodes. The presence of a chemical additive known to shift the equilibrium of the two-phase system can merge droplets in the confinement.[20] In this work, we used 40% (v/v) octanol in mineral oil due to its insolubility in water. A 1 : 1 merging of droplets occurred in 83% of the wells (Fig. 2e). The open structure of the mesh grid also allows selective recovery of droplets from the array using a glass capillary tube (Fig. 2f).

Fig. 3a shows the first trap of droplets transferred from the second breakup channel to the array, filling 48% of the microwells with single cells (see green fluorescence inside droplets). Fig. 3b is the result of the addition and merging of the second droplets containing red fluorescent cells, demonstrating that the array can be used to co-encapsulate two different cells. The green and red fluorescent cells were *E. coli* expressing green fluorescent protein (EGFP) and red fluorescent protein (DsRed2), respectively. The top of the droplet array was covered with mineral oil to prevent evaporation, and supplementary medium droplets were added to the array at 1 h intervals throughout the events. By removing a droplet from the array and transferring it to a solid agar plate, we could recover the target cell and grow it into a colony (see ESI, Fig. S3†).

We examined the applicability of the mesh-integrated array for single-cell-based reactions by merging droplets containing specific enzyme (tyrosine phenol-lyase)-producing *E. coli* with the second droplets of reporter cells. The reporter cells are *E. coli* genetically modified to emit green fluorescence in the presence of the enzyme product (phenol), which is released from the enzyme-producing cells (see ESI, Fig. S4 and S5†). Thus, when two droplets merge, green fluorescence is produced, indicative of the enzyme reaction (Fig. 3c). When the numbers of both enzyme-producing cells and reporter cells per droplet are as many as 5–10, those multiple cells will produce more enzyme and product within the same confinement, resulting in a greater fraction of reacted droplets in the array (Fig. 3d). Less than 10% of the microwells showed reactions in the single-cell droplet array, in which the numbers of both enzyme-producing cells and reporter cells were controlled to be single in each droplet. In this confinement, at least 3 h of incubation was required for sufficient accumulation of product and detection of reporter cells at the single-cell level. With the small scale of the droplet confinement, designed for instant analysis of single-cell units, a period of 5 h was adequate to monitor fluorescence intensity from cell-to-cell reactions. Longer incubation times increase the proportion of droplet loss from evaporation.

The mesh-integrated droplet array provides a microfluidic platform for simple storage and on-demand merging of droplets. The openness of the system allows easy access to individual droplets and variable integration with other functional modules. By integrating the single-cell droplet-generating channel, the mesh-integrated microarray allows immediate confinement of single cells and total isolation of each chamber throughout the entire droplet manipulation process. With further development of cell-friendlier conditions and automation for parallel handling of droplets, this device may provide a novel screening platform, especially for various microbes directly harvested from a natural environment.

This research was supported by the National Leading Research Laboratory Program grant (no. 2011-0018607) through the National Research Foundation of Korea (NRF). S.-G.L. acknowledges the Global Frontier Program grant (no. 2011-0031944) for the intelligent synthetic biology by the NRF for financial support. The authors also acknowledge Joonwoo Jeong and Gil-Gwang Kwon for experimental support and discussion.

References

1 S. Lindstrom and H. Andersson-Svahn, *Lab Chip*, 2010, **10**, 3363–3372.
2 A. D. Tadmor, E. A. Ottesen, J. R. Leadbetter and R. Phillips, *Science*, 2011, **333**, 58–62.
3 J. Q. Boedicker, M. E. Vincent and R. F. Ismagilov, *Angew. Chem., Int. Ed.*, 2009, **48**, 5908–5911.
4 L. Kang, M. J. Hancock, M. D. Brigham and A. Khademhosseini, *J. Biomed. Mater. Res., Part A*, 2010, **93**, 547–557.
5 M. C. Park, J. Y. Hur, K. W. Kwon, S.-H. Park and K. Y. Suh, *Lab Chip*, 2006, **6**, 988–994.
6 Y. Tokimitsu, H. Kishi, S. Kondo, R. Honda, K. Tajiri, K. Motoki, T. Ozawa, S. Kadowaki, T. Obata, S. Fujiki, C. Tateno, H. Takaishi,

K. Chayama, K. Yoshizato, E. Tamiya, T. Sugiyama and A. Muraguchi, *Cytometry, Part A*, 2007, **71**, 1003–1010.
7 J. Clausell-Tormos, D. Lieber, J.-C. Baret, A. El-Harrak, O. J. Miller, L. Frenz, J. Blouwolff, K. J. Humphry, S. Köster, H. Duan, C. Holtze, D. A. Weitz, A. D. Griffiths and C. A. Merten, *Chem. Biol.*, 2008, **15**, 427–437.
8 E. Um, D.-S. Lee, H.-B. Pyo and J.-K. Park, *Microfluid. Nanofluid.*, 2008, **5**, 541–549.
9 C. Priest, S. Herminghaus and R. Seemann, *Appl. Phys. Lett.*, 2006, **89**, 134101.
10 H. Song, D. L. Chen and R. F. Ismagilov, *Angew. Chem., Int. Ed.*, 2006, **45**, 7336–7356.
11 E. Um and J.-K. Park, *Lab Chip*, 2009, **9**, 207–212.
12 J.-u. Shim, L. F. Olguin, G. Whyte, D. Scott, A. Babtie, C. Abell, W. T. S. Huck and F. Hollfelder, *J. Am. Chem. Soc.*, 2009, **131**, 15251–15256.
13 P. Abbyad, R. Dangla, A. Alexandrou and C. N. Baroud, *Lab Chip*, 2011, **11**, 813–821.
14 M. Sun, S. S. Bithi and S. A. Vanapalli, *Lab Chip*, 2011, **11**, 3949–3952.
15 A. C. Hatch, J. S. Fisher, A. R. Tovar, A. T. Hsieh, R. Lin, S. L. Pentoney, D. L. Yang and A. P. Lee, *Lab Chip*, 2011, **11**, 3838–3845.
16 E. Brouzes, M. Medkova, N. Savenelli, D. Marran, M. Twardowski, J. B. Hutchison, J. M. Rothberg, D. R. Link, N. Perrimon and M. L. Samuels, *Proc. Natl. Acad. Sci. U. S. A.*, 2009, **106**, 14195–14200.
17 A. Huebner, M. Srisa-Art, D. Holt, C. Abell, F. Hollfelder, A. J. deMello and J. B. Edel, *Chem. Commun.*, 2007, 1218–1220.
18 S. Köster, F. E. Angile, H. Duan, J. J. Agresti, A. Wintner, C. Schmitz, A. C. Rowat, C. A. Merten, D. Pisignano, A. D. Griffiths and D. A. Weitz, *Lab Chip*, 2008, **8**, 1110–1115.
19 E. Um, S.-G. Lee and J.-K. Park, *Appl. Phys. Lett.*, 2010, **97**, 153703.
20 K. Larson, B. Raghuraman and J. Wiencek, *J. Membr. Sci.*, 1994, **91**, 231–248.